Journal of the Chinese Chemical Society, **1995**, *42*, 293-302

Reaction Dynamics of $Mg(3s3p\,^1P_1)$ with H_2

Dean-Kuo Liu (劉定國), Thou-Long Chin (覃昭龍), Yaw-Ren Ou (歐耀仁),
Cheng-Tsung Huang (黃正宗) and King-Chuen Lin* (林金全)
Department of Chemistry, National Taiwan University and Institute of Atomic and Molecular Sciences, Academia Sinica, P.O. Box 23-166, Taipei, Taiwan 10764, Republic of China

We measured the temperature dependence of rotational population distribution of the nascent product $MgH(^2\Sigma^+)$ in the reaction of $Mg(3s3p\,^1P_1)$ with H_2. The results indicate that the reaction is dominated by an Mg-insertive mechanism, consistent with the isotope effect reported previously. We also presented the vibrational population distribution, and thereby found that two parallel reaction pathways are responsible for the subject reaction following Mg-H_2 collision in a bent configuration. The major one produces MgH in higher rotational levels and comparable $v'' = 0$ and $v'' = 1$ populations, while the other minor one produces MgH in low rotational levels and preferentially $v'' = 0$. By means of a two-dimensional potential energy surface(PES) calculation, a deep insight into the reaction pathways has been gained. The resulting PES's information reveals the possibility of a nonadiabatic transition between the excited $^1B_2$ PES and the ground PES. The bent intermediate MgH_2 near the surface crossing starts trajectories either smoothly following the dissociation coordinate of Mg-H distance or attractively falling down through a linear HMgH geometry before breaking apart. The former trajectory accounts for the minor reaction pathway to produce MgH, while the latter one responses to the major reaction pathway. The impact of isotope and temperature effects on MgH can also be readily explained with use of the calculated PES's.

INTRODUCTION

The reaction dynamics of the excited Mg* atom with the H_2 molecule have been investigated for decades, and deep insight into the reaction has been gained.[1] For instance, there has become available information on energy surfaces and potential barriers for the reaction,[2-4] state-to-state quenching cross sections,[5-7] effective reaction orientation between Mg* and H_2,[2,3,8-10] probing of the transient intermediate MgH_2,[11-13] as well as the energy distribution of the subsequent product MgH.[8,9,14] These achievements are ascribed notably to the use of pump-and-probe technique, which has made access to a single collisional event possible under bulk conditions.[8,11,14-16] In this dual-laser technique, one laser is utilized to initiate the reaction, followed within a few nanosecond delay by the other laser which is capable of monitoring the status of the product. The delay interval can be adjusted to such extent that the nascent product may avoid relaxation caused by secondary collisions. Therefore, the study of correlation of the energy distribution of the product with the collision orientation becomes possible even under the bulk cell condition.

By using such a pump-and-probe method in the study of reaction

$$Mg(3s3p\,^1P_1) + H_2 \rightarrow MgH(v'', N) + H, \qquad (1)$$

Breckenridge *et. al.* have demonstrated that the rotational population distribution of the nascent product $MgH(v'' = 0)$ was characterized by a bimodality.[8] Two parallel reaction mechanisms of insertion and abstraction was proposed previously. The large component over the higher rotational quantum states was considered to follow a mechanism of Mg insertion into the H_2 bond by a side-on attack. As one H atom escapes from the bent intermediate MgH_2, a rotational torque is exerted upon the remaining MgH, leading to population distribution in the higher rotational quantum states. In contrast, a small portion of lower rotational energy distribution was proposed to proceed with a reactive approach having a collinear configuration. Thus the mechanism of H-abstraction by the end-on attack may not impact on the rotational energy of MgH significantly.[8] In a recent investigation of probing the transient intermediate MgH_2 with use of matrix isolation method at 12K, McCaffery *et al.* have identified the linear structure H-Mg-H to be the only stable configuration.[13] They safely ruled out the possibility of "cage effect", which may facilitate the recombination of MgH and H, the fragments resulting from the H-abstraction pathway. This fact suggests that MgH + H product in the gas-phase reaction should result from the reactive approach of Mg-insertion, to the contrary of the results previously reported.[8] In addition, Breckenridge *et al.* using isotopic hydrogens as reagents showed a profile coincidence of rotational state distribution of $MgH(v'' = 0)$ produced either from HD or H_2.[9]

The lack of a significant isotopic effect also suggested that the bimodality may originate from a single mechanism. They therefore concluded that eq. (1) is an exit-channel controlled reaction, which is dominated by the insertive mechamsm.

Although a profound insight into the reaction (1) has thus been gained, the detailed pathways leading to the rotational bimodality are still questionable. It is believed that this reaction is exit-channel controlled, forming the MgH product through two distinct pathways; one corresponds to the high N component of the rotational state distribution, and the other is relevant with the low N state distribution. If the insertive mechanism dominates the reaction (1), and accounts for the high N component of the distribution, what mechanism may be responsible for the low N component? From the theoretical point of view, Chaquin *et. al.* have suggested that the electronic state $^1B_2$—$^3A_1$ surface crossing may explain the formation of the small low N component of the distribution.[3] The $^3A_1$ surface correlates with the ground electronic state of linear structure Mg-H-H, from which the terminal H atom escapes without causing significant rotational excitation of MgH. However, Mg doesn't seem to be heavy enough to induce effectively the spin-orbit coupling between these two states; the corresponding emission of the $3^3P \rightarrow 3^1S$ transition was not yet observed.[9] It is apparently of vital importance for a thorough investigation into eq. 1 to unveil the reaction pathways associated with it.

In order to clarify the ambiguity on H-abstractive vs Mg-insertive mechanisms encountered in the reaction(1),[8,9,13] in the paper we present alternatively an experiment of temperature dependence of product rotational state distribution.[10] Because the potential barriers differ between the collinear and the bent collisional conformations,[3] these two reactive mechanisms are expected to respond differently to the effect of temperature. Thereby determination of the predominant mechanism becomes feasible. We also report a detailed information on the vibrational state distribution associated with eq. (1), which appears to be conducive to a deep understanding of the reaction dynamics. We found that the rotational population distributions in both $v'' = 0$ and 1 states herein appear to be bimodal. The two components contained may be deconvoluted with use of the linear surprisal method. The minor "low N" component of the distribution in the $v'' = 0$ state is larger than that in the $v'' = 1$ state, whereas the major "high N" component of the distribution becomes roughly equivalent to that in the $v'' = 1$ state.[14] Two parallel pathways are then expected to be relevant with the reaction dynamics. One type produces MgH in low rotational levels and preferentially $v'' = 0$, and the other type produces MgH in higher rotational levels with comparable $v'' = 0$ and $v'' = 1$ populations. Note that the previous interpretation of the reaction pathways for the rotational bimodality is essentially based on the impulsive model,[8,9,10,14] which assumes that in a three-particle system the departing atom and the remaining diatom break apart abruptly depending upon the initial bonding angle. The model ignores the influence of angle variation along the reaction coordinate, and oversimplifies the treatment of potential interaction using a diatomic potential term instead of a real potential energy surface(PES). In order to avoid the mistake probably made with this model, we provide a two-dimensional PES calculation for the excited and ground states involved in the reaction.[4] The results support the possibility of the nonadiabatic transition in the production of MgH,[3,14] and yield detailed information, on which bimodal nature,[8,14] isotope effect,[9] and temperature dependence[10] of the product rotational population distribution may be successfully interpreted.

EXPERIMENTAL

The pump-and-probe technique used in this work has been illustrated previously[10,14,17,18] and described in detail elsewhere.[8,11] Briefly, the pump-and-probe technique, as shown in Fig. 1, employed two dye lasers which were pumped, respectively, by a frequency-doubled and a frequency-tripled 10 Hz, 5-8 ns Nd:YAG laser. The pump laser was operated with mixed dyes of Rhodamine 590 and Rhodamine 610. The tunable output near 570 nm was frequency doubled by passage through a KD*P crystal and converted to 285 nm, which excited the Mg atomic vapor to the 3^1P_1 state. The laser energy was low enough to ensure that a one-photon excitation process was involved. The resulting MgH

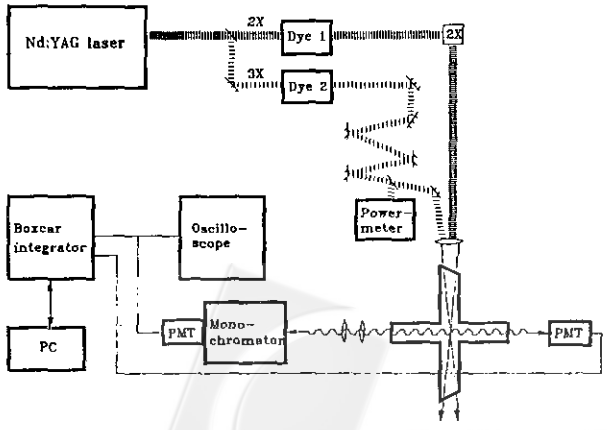

Fig. 1. Schematic diagram of the pump-and-probe experimental apparatus.

product was monitored with laser-induced fluorescence(LIF) in the $A^2\Pi$—$X^2\Sigma^+$ band using a probe laser with less than a 20 ns delay with respect to the pump laser. Given the H_2 pressure in the chamber in the range of 0.5-4 Torr, the delay time was adjusted to the extent so that the MgH observed was collision free. Both lasers propagated collinearly and their powers were monitored continuously with an individual photodiode. The energy of the unfocused pump beam was 100-400 μJ for $Mg(^1P_1)$ excitation, while the unfocused probe beam was about 100 μJ.

The obtained LIF signal of (0,0) and (0,1) bands ((v′, v″) notation used) was focused by means of two lenses onto a monochromator. The center wavelength of the grating was set to 560 nm and 517 nm, respectively, for the $v' = 0 \rightarrow v'' = 1$ and $v' = 0 \rightarrow v'' = 0$ transitions. As the slits were 5 mm wide, the monochromator with dispersion 1.8 nm/mm acted as an interference filter having 9 nm bandpass. Thus the transmitted LIF signal was detected by an attached photomultiplier tube. The signal was processed by a boxcar integrator and then normalized to the condition of the identical power of laser irradiation. A microcomputer interfaced to the boxcar integrator stored the data for further treatment.

The reaction chamber was a stainless steel five-armed cross heat-pipe oven, allowing for spectral observation perpendicular to the laser axis.[10,11,14,17] A thermocouple, inserted through the top arm in the vicinity of the reactive region, was used to monitor the oven temperature with an accuracy ± 1K. The Mg metal was deposited and heated to 680—760 K, corresponding to a vapor pressure of 3—50 mTorr. The pressure of gaseous H_2 in the oven was maintained from 0.5 to 4 Torr with an MKS Baratron manometer.

COMPUTATION PROCESS

For performing two-dimensional PES calculation of bent intermediate MgH_2 as functions of bending angle and bond length, we adopted the basis sets in 6-31G** level for Mg and H atoms. CI calculation with single excitation (CIS) contained in the Gaussian 92 package of program[19] was used to compute the excited state $^1B_2$ of $Mg(^1P_1) + H_2$, which correlates symmetrically with the final products of $MgH(^2\Pi) + H$. The fourth-order Møller-Plesset (MP4) method was used for the PES calculation of the ground state $^1A_1$ of $Mg(^1S_o) + H_2$, which correlates symmetrically with the $MgH(^2\Sigma^+) + H$ products. The perturbative technique adopted the HF/6-31G** structure as the previous run. A single point calculation was performed over at least 625 configurations each for the two-dimensional PES's of excited and ground states. To test reliability of the methods used, structure optimization of MgH ($^2\Pi$ and $^2\Sigma^+$) and linear HMgH ($^1\Pi_g$ and $^1\Sigma^+_g$) were computed, and the results of their bond lengths and total absolute potential energies are in agreement with those reported previously.[3,20-22]

RESULTS AND DISCUSSION

Laser-induced Fluorescence Spectra of MgH

The LIF spectra of the (0,0) and (0,1) bands in the $A^2\Pi$—$X^2\Sigma^+$ transition of the nascent MgH product were obtained following excitation of $Mg(^1P_1)$ at 285.2 nm. The rotational lines of N = 1-10 and 21-30 for the P branch in the (0,0) band, and those of N = 1—7 and 15—27 in the (0,1) band can be resolved completely under our laser conditions with resolution ≤ 1 cm^{-1}. However, the N = 11—20 lines of the (0,0) band and the N = 8—14 lines of the (0,1) band overlap severely, so that a computer simulation is applied to obtain the deconvoluted spectra.[8,10,14] A satisfactory agreement between the simulated spectra and the LIF spectra of the (0,1) band is revealed in Fig. 2. Note that the Q and R branches in the (0,1) band have onsets close to the P branch with N ≥ 20, and therefore they may interfere significantly with the high N component of the P branch. With the Q and R branches taken into account in the simulation, fortunately several high N rotational lines such as $P_1(21)$, $P_1(22)$, $P_1(24)$, $P_1(25)$, $P_1(26)$ and $P_2(27)$ may be resolved from the Q and R branches, and their intensities can be estimated within a small error. Because of the good spectral resolution, the P_1 branch is selected for determination of the rotational distribution.

For detecting the population in the $v'' = 0$ state, the (0,0) band is excited while the emission band of (0,1) is monitored. In contrast, for detecting the population in the $v'' = 1$ state, the (0,1) band is excited and then the (0,0) band is monitored. Although the Franck-Condon factor for the $v'' = 1 \rightarrow v' = 0$ excitation transition is about an order of magnitude smaller than that of transition $v'' = 0 \rightarrow v' = 0$, the small transition probability is compensated by monitoring a strong emission band (0,0). Accordingly, while comparing the total population between the $v'' = 0$ and $v'' = 1$ states, there is no need to take into account the Franck-Condon factor for correction.

Analysis of Rotational State Distribution

In the electronic transition $A^2\Pi$—$X^2\Sigma^+$ of MgH, the ground state belongs to Hund's case (b), while the $A^2\Pi$ state is considered to be a case intermediate between (a) and (b). Hund's case (b) dominates with increasing N, causing spin-decoupling with the molecular axis. However, Hund's case

(a) becomes important for those low N rotational lines, depending upon the ratio of A/B_v, in which A denotes the coupling constant between the spin and the orbital angular momentum and B_v is the rotational constant.[23] The value of A/B_v is indicative of the strength of the spin coupling to the molecular axis. When the ratio approaches to zero, the transition type belongs to Hund's case (b), whereas it tends to be close to Hund's case (a) as the ratio approaches to $\pm\infty$. For the case of MgH, the values of A and B_v are 35.3 and 6.09 for $v'' = 0$, respectively, and thus the ratio equals to 5.8. For such an intermediate case, the intensity of the four satellite transition lines ($^PQ_{12}$, $^RQ_{21}$, $^QR_{12}$ and $^QP_{21}$) are not negligible, especially in the low N region. The only satellite branch that may disturb the assigned P_1 and P_2 lines is $^PQ_{12}$, of which the wavelength difference from the P_1 branch depends upon the spin-splitting between the doublets of the $X^2\Sigma^+$ state. Because the spin-splitting constant is as small as 0.025 cm^{-1},[23] the satellite branch $^PQ_{12}$ occurs essentially at the same frequency as the P_1 branch under our laser conditions. According to the Hönl-London formula derived by Earls,[24] the intensities of rotational lines of the P_1 branch are estimated to be 0.167, 0.391, 0.633, 0.880 and 1.13 for N = 1,2,3,4 and 5, respectively, while the intensities of the $^PQ_{12}$ satellite branch are estimated to be 0.333, 0.205, 0.149, 0.115 and 0.093. The ratio of $P_1(N)/^PQ_{12}(N)$ increases rapidly with increasing the quantum number N, and therefore the observed intensities of the P_1 lines that may be masked significantly by the satellite branch are limited within a few low N states.

By taking into account the Hönl-London factor and intensity correction with subtraction of the satellite $^PQ_{12}$, from the observed P_1 branch, the rotational state distributions of MgH in the $v'' = 0$ and 1 states appear to be bimodal. As shown in Figs. 3 and 4, both population distributions are represented by the P_1 branch, which turns out to be less overlapped spectrally in the high N component especially for the (0,1) band. The rotational population distribution in the $v'' = 0$ state, represented by the P_1 branch, is consistent with those reported by Breckenridge *et. al.*[8,9] using the average of the P_1 and P_2 branches instead. By summing up the population intensity of each rotational line, our measurement of population ratio of $MgH(v'' = 1)/MgH(v'' = 0)$ reaches 0.8 ± 0.1, in agreement with the value of 0.7 ± 0.2 obtained by Breckenridge *et. al.*[8]

Although their determined ratio of $MgH(v'' = 1)/MgH(v'' = 0)$ is consistent with ours,[8] the treatment of Breckenridge and his co-worker by computer simulation to find the $MgH(v'' = 1)$ population distribution is less reliable. They determined the rotational state distribution of $MgH(v'' = 1)$ by monitoring emission of the (1,0) band following excitation of the (1,1) band.[8] The excitation spectrum of the (1,1) band is severely blended by the P_1, P_2, Q_1, Q_2, R_1, and

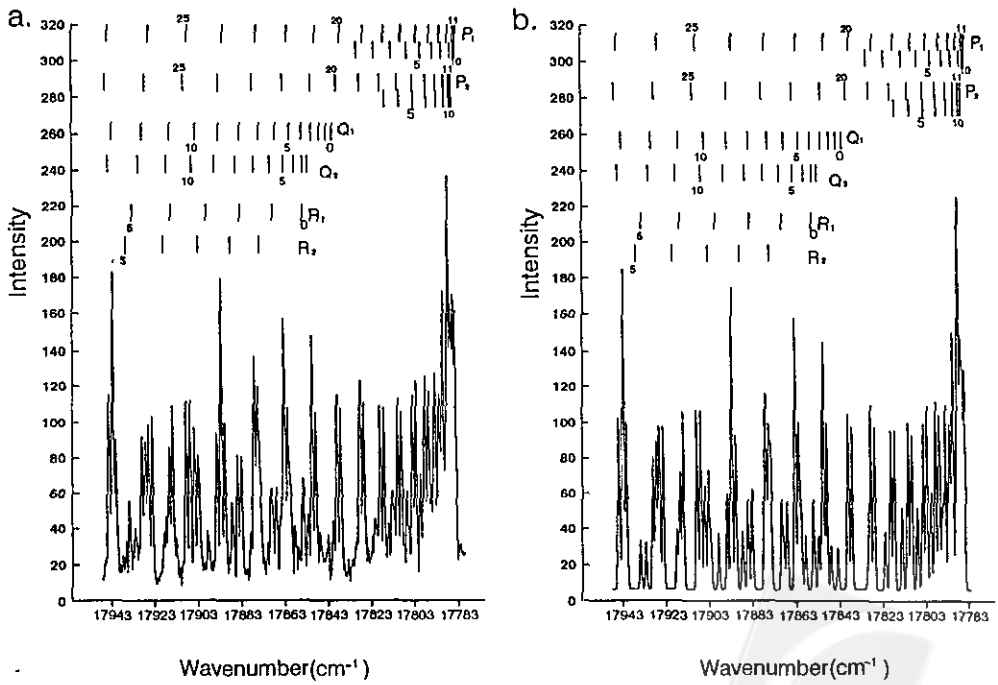

Fig. 2. (a) A portion of LIF spectra for the P, Q and R branches in the (0,1) band of the $MgH(A^2\Pi—X^2\Sigma^+)$ transition. (b) Spectra by computer simulation of the same region. $MgH(v'' = 1)$ is a nascent product in the reaction of $Mg(^1P_1)$ with H_2. Computer-simulated spectra can best fit the experimental result.

R_2 branches of the (0,0) band. It is insensitive and less reliable to extract information on the $v'' = 1$ population from such a congested spectrum.[14] In contrast, the rotational spectrum of MgH in the (0,1) band is well resolved up to N = 27 for the P branch except for the lines around the bandhead, of which the resolution relies upon the computer simulation. In addition, the small N component has been corrected for its intensity by considering the contribution of satellite $^PQ_{12}$. The rotational population distribution in the $v'' = 1$ state obtained in this work is apparently more acceptable.

With use of linear surprisal method,[25] the high N component of the rotational population distribution of MgH($v'' = 0$ and 1) can be fitted satisfactorily, and thus the small, low N component may be deconvoluted as shown in Fig. 5. As compared with the rotational population distribution of MgH($v'' = 0$), MgH($v'' = 1$) is found to have an equivalently great distribution for the high N component, but a smaller distribution for the low N component. The population ratio of MgH($v'' = 1$)/MgH($v'' = 0$) gives a individual value of 0.42 ± 0.05, and 0.87 ± 0.05 for the low N component and the high N component, respectively. Accordingly,we expect that parallel reaction pathways are associated with the subject reaction. The major one produces MgH in higher rotational levels and comparable $v'' = 0$ and $v' = 1$ populations, and the other minor one produces MgH in low rotational levels and preferential vibrational state at $v'' = 0$.

Temperature Effect: Abstraction vs Insertion

In the experiment of the temperature dependence, the rotational state distribution of MgH($v'' = 0$) obtained at 733 K was normalized and compared with that at 693K, as well as with the results at 380 K by Breckenridge and Umemoto.[8] As shown in Fig. 6, the bimodal profiles are coincident satisfactorily within the experimental error. Note that, for comparison with the results reported ,the average of the P_1 and P_2 branches in the (0,0) band is adopted correspondingly for the rotational state distribution. The results in Fig. 6 also make little difference from the bimodal profile shown in Fig. 5, in which only P_1 branch is considered.

In the calculation of dynamical PES for the reaction of $Mg(^1P_1)$ with H_2, Chaquin *et. al.* reported the reaction barriers for the cases of collinear ($C_{\infty v}$) and bent (C_{2v}) configurations, corresponding to an end-on or side-on approaches in Mg-H_2 collision.[3] As the insertive reaction occurs to form a bent MgH_2 intermediate, the reaction coordinate tracks an attractive $^1B_2$ surface without suffering from any activation barrier. In contrast, a collinear approach leads to a barrier as large as 1.8 or 1.7 eV as either a $^1\Sigma^+$ or a $^1\Pi$ surface is followed, respectively. Presumably the bimodal nature of the MgH product is ascribed simultaneously to both end-on and side-on attacks, then these two reaction mechanisms may re-

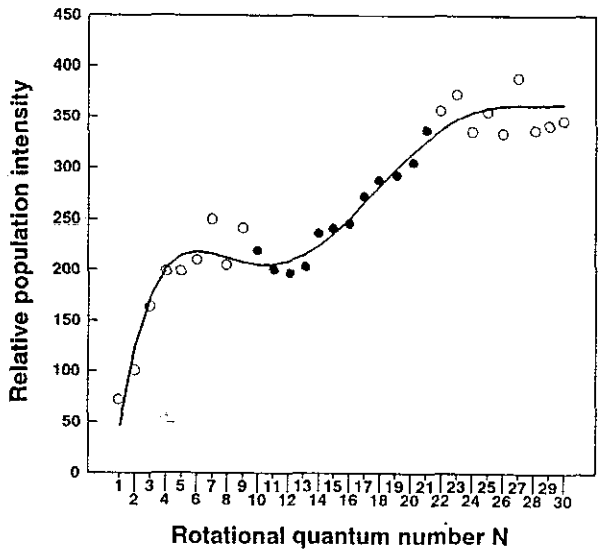

Fig. 3. Rotational population distribution of MgH in the $v'' = 0$ state. The open circles denote the experimental finding of the P_1 branch; the closed circles denote the deconvoluted spectra around the bandhead by computer simulation. The solid line is the least-squares fit based on a sixth power polynomial.

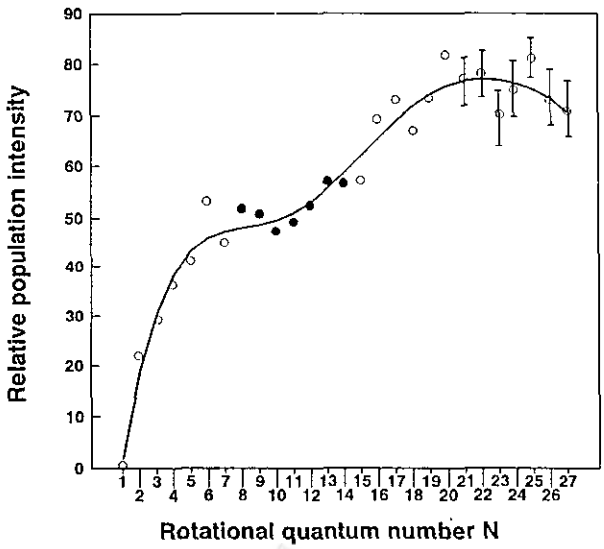

Fig. 4. Rotational population distribution of MgH in the $v'' = 1$ state. The open circles denote the experimental finding of the P_1 branch; the closed circles denote the deconvoluted spectra around the bandhead by computer simulation. The solid line is the least-squares fit based on a sixth power polynomial.

spond differently to the temperature effect, since the barrier differs for MgH produced between collinear and bent colliding geometries. If a reaction coordinate follows the repulsive potential surface in the entrance channel geometry, according to the Arrhenius theory, the rate of formation of the product is expected to increase with increasing temperature. If the reaction proceeds without an energy threshold, the reaction rate decreases with increasing temperature; the prediction of temperature effect based on a transient complex model, which has been successfully employed to interpret an unusually large quenching cross section, is consistent with this absence of an energy threshold.[26-28] The intermediate complex formed by the substrate and the quencher is dominated by the attractive long-range interaction in the entrance coordinate. With increased temperature, the lifetime of the complex decreases such that the energy originally deposited in the substrate cannot be significantly transferred to all possible exit channels. The resulting quenching rate appears to decrease as temperature increases. Accordingly, the temperature dependences of the abstractive and insertive reactions show opposite influence upon the low N and high N components of the rotational distributions, respectively.

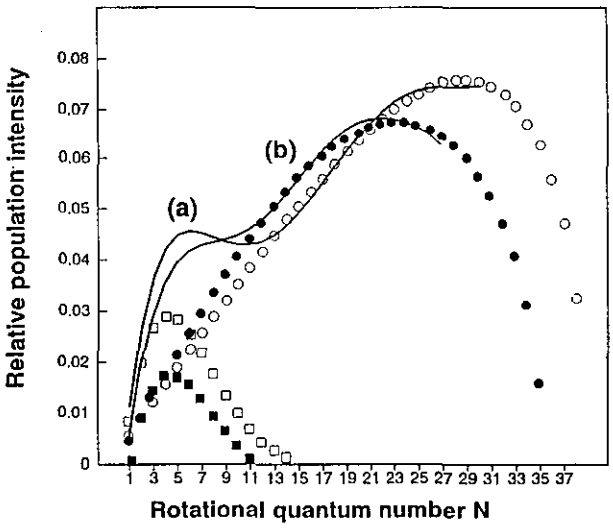

Fig. 5. Solid lines, (a) and (b) indicated the nascent rotational population distribution of MgH in the v″ = 0 and v″ = 1 state, respectively, as determined in Figs. 3 and 4. Closed circles, the high N component of MgH(v″ = 1) fitted using linear surprisal method. Closed squares, the low N component of MgH(v″ = 1) deconvoluted from subtraction of solid line(b). Open circles, the high N component of MgH(v″ = 0) fitted using linear surprisal method. Open squares, the low N component of MgH(v″ = 0) deconvoluted from subtraction of solid line(a).

The lack of temerature effect in the range 380 - 733 K on the MgH rotational population distribution confirms that the reaction is initiated only by insertion, in agreement with the conclusion drawn from the isotope effect. However, we believe that the former method is more effective than the latter for examining contribution of abstraction/insertion to the subject reaction. The isotopic hydrogen effect depends essentially upon the ratio of H to D, which is limited within a small value.[29-31] In some cases the ratio happens to have small difference from the unity, such that the effect becomes insignificant. Because the temperature may be varied continuously, the temperature dependence, unlike the isotope effect, can magnify remarkably the difference between the rotational state distributions, if both insertion and abstraction have contributions.

PES Information: Reaction Pathways

The reaction pathways for the Mg($^1P_1$)-H_2 collision proposed previously are rather ambiguous.[3,8,9,14] It is believed that two parallel mechanisms are responsible for the rotational bimodality following Mg insertion towards the H_2 molecule to form a bent configuration. For the small N component, Chaquin *et. al.* suggests that the reaction coordinate along the $^1B_2$ state may cross the $^3A_1$ surface, which correlates with the linear configuration of Mg-H-H.[3] If such a singlet-to-triplet surface crossing does happen, the kinematic effect may cause a hot vibrational motion and a cold rotational excitation for MgH. The interpretation is apparently against our experimental findings of MgH, which is

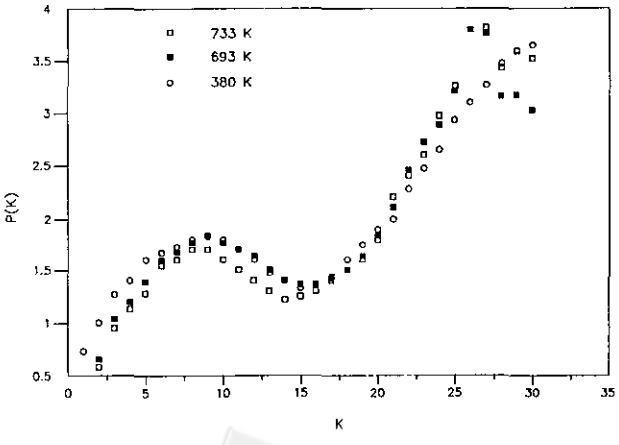

Fig. 6. A comparison of normalized,bimodal population distribution for the nascent product MgH under various temperature conditions. (■) and (□) denote the results in this work taken at 683 and 733 K, respectively; (o) denotes the result of 380 K from the work of Breckenridge and coworkers.

populated in low N state distribution and preferentially v″ = 0. On the other hand, the high N component of the distribution is expected previously to follow a mechanism, in which the H atom departs from a bent intermediate MgH_2.[3,8,9,14] Assuming that the H-H interaction is much stronger than the H-Mg interaction, then a torque generated according to the impulsive model[32] may cause MgH to be excited rotationally. This discussion somehow neglects consideration of the isotope effect. If the assumption is acceptable, HD, as used to replace H_2, may cause a different product rotational state distribution, which is against the observation of Breckenridge *et. al.*[9]

For providing a deep insight into the reaction pathways associated with the subject reaction, we present a detailed PES calculation.[4] Fig. 7 shows the two-dimensional PES's in the $Mg(^1P_1)$-H_2 reaction for the ground and excited states as functions of the bending angle α and the bond distance between Mg and the departing H atom, while the other MgH bond is fixed at 1.7345 Å, equilibrium distance calculated for the ground state of MgH. The ground and excited PES's associated with the $Mg(^1S_0) + H_2$ and $Mg(^1P_1) + H_2$ reactants correlate symmetrically with the asymptote states of $MgH(^2\Sigma^+) + H$ and $MgH(^2\Pi) + H$, respectively. The angle is varied between 35 and 59°, and the bond distance ranges from 1.2 to 3.96 Å.

The upper and lower PES's happen to cross mainly at two regions. A detailed description of the surface crossing is given in Fig. 8, showing the projection of the surface crossing on the equipotential contour of the ground PES. Two main features appear in this equipotential contour plot. Firstly, as one may see, the ground PES is steeply repulsive at Mg-H distance short near 1.2 Å, and gradually slides down along the dissociation direction of Mg-H coordinate. Secondly, as the Mg-H distance is close to 1.7 Å and the angle exceeds about 50°, the PES begins to show a strong angular dependence; with increasing the bending angle to 180°, the potential surface rapidly falls down to the well, ~3.8 eV below the reference energy of the $Mg(^1P_1) + H_2$ reactants. Two crossing regions are indicated in the figure. One (denoted as A) is surrounded within the range of $47° \le \alpha \le 53°$ and $1.6\ Å \le r \le 2.0\ Å$, and the other(denoted as B) is within $52° \le \alpha \le 55°$ and $2.2\ Å \le r \le 2.7\ Å$. The structure of intermediate MgH_2 near the region A is close to a C_{2v} geometry having approximately equal bond distance; in contrast, the structure near the region B appears a Cs geometry with one bond fixed at 1.7345 Å and the other stretched up to 2.7 Å.

As discussed in the preceding section, the collision of $Mg(^1P_1)$ with H_2 follows the attractive $^1B_2$ surface and ends in the production of $MgH(^2\Sigma^+) + H$. To obtain the MgH in the $^2\Sigma^+$ state, the nonadiabatic transition between the excited and ground PES's has to take part in the reaction. Although the transition probability of surface crossing is unknown, a larger probability is expected to occur at the region of Cs geometry. A Cs symmetric structure of intermediate MgH_2 may enhance the coupling strength between the bending mode and the asymmetric stretching mode ($^1b_2$), which

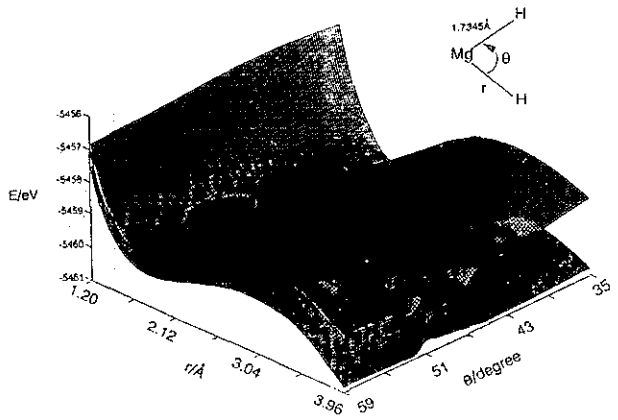

Fig. 7. Two-dimensional PES's as function of bending angle and bond distance of excited and ground states associated with the reaction of $Mg(^1P_1)$ with H_2, under the condition that one MgH bond is fixed at 1.7345 Å. The excited PES follows the $^1B_2$ surface, correlating symmetrically with $MgH(^2\Pi) + H$, while the ground PES follows $^1A_1$ surface, correlating symmetrically with $MgH(^2\Sigma^+) + H$.

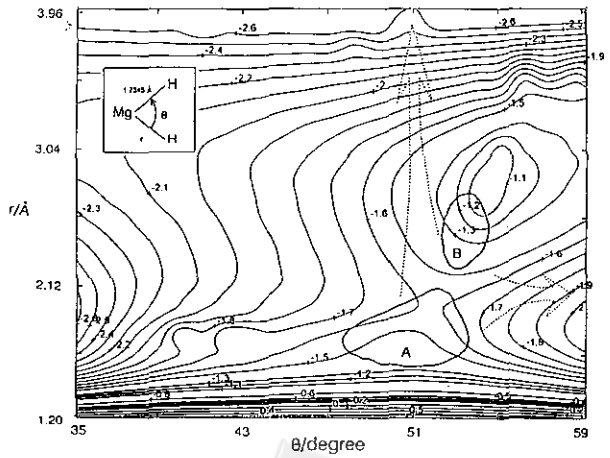

Fig. 8. Projection of surface crossings (in Fig. 7) on the equipotential contour of ground PES with the relative energy in eV. The heavy circles denote the surface crossing regions. The arrows are indicative of the possible exit-channel directions for departing of H atom from the bent intermediate near the crossing regions.

needs to be involved to induce a vibronic transition;[14] the $^1B_2$ - $^1A_1$ crossing transition is otherwise forbidden. For this reason, the surface crossing at region B is expected to have a larger transition probability than that at region A.

With use of a Jacobi coordinate to define the intermediate geometry near the crossing region for the Mg-H_2 collision, R denotes the distance between the departing H atom and the center of mass of MgH product, r is the bond length of MgH, and θ is the Jacobi angle between R and r axes.[32] Since the center of mass of MgH is positioned almost on the Mg atom, the Jacobi angle is approximately equal to the bond angle. The variation of the rotational angular momentum in time is related to the torque generated, as expressed in the following,[32-33]

$$\frac{dj}{dt} = \frac{\partial V(\theta,R)}{\partial \theta} \qquad (2)$$

The equation indicates that the rotational excitation depends upon the anisotropy of the relevant PES.

From the equipotential contour plot of the ground PES (Fig. 8), one may expect that the intermediate MgH_2 at the crossing regions starts trajectories either smoothly following the dissociation coordinate of Mg-H distance or attractively falling down through the linear HMgH geometry before breaking apart. If the removal of H from the intermediate is along directly the dissociation coordinate of Mg-H, as pointed by the arrow in Fig. 8, the trajectory causes apparently insignificant rotational excitation; according to eq. 2, the angular dependence of the potential is very weak. Note that the dissociation process also results in little change of the MgH bond length. This fact suggests that the R and r coordinates are weakly coupling during the dissociation. The final MgH product is predicted apparently to be in the low quantum states of rotation and vibration. In contrast, when the bent intermediate is attracted substantially following a trajectory through the linear geometry (Fig. 8), according to eq. 2, a strong angular dependence of the PES results in a large torque, which gives rise to rotational and vibrational excitation. The reaction pathways are depicted in Fig. 9. The former reaction pathway accounts for our experimental findings for MgH which appears in low rotational states and preferentially $v'' = 0$, while the latter one leads to rotational and vibrational excitation of MgH product observed.[4,14]

With information on the intermediate geometry at the surface crossing, one may readily interpret why the isotope effect on MgH,[9] as produced by reaction either with H_2 or

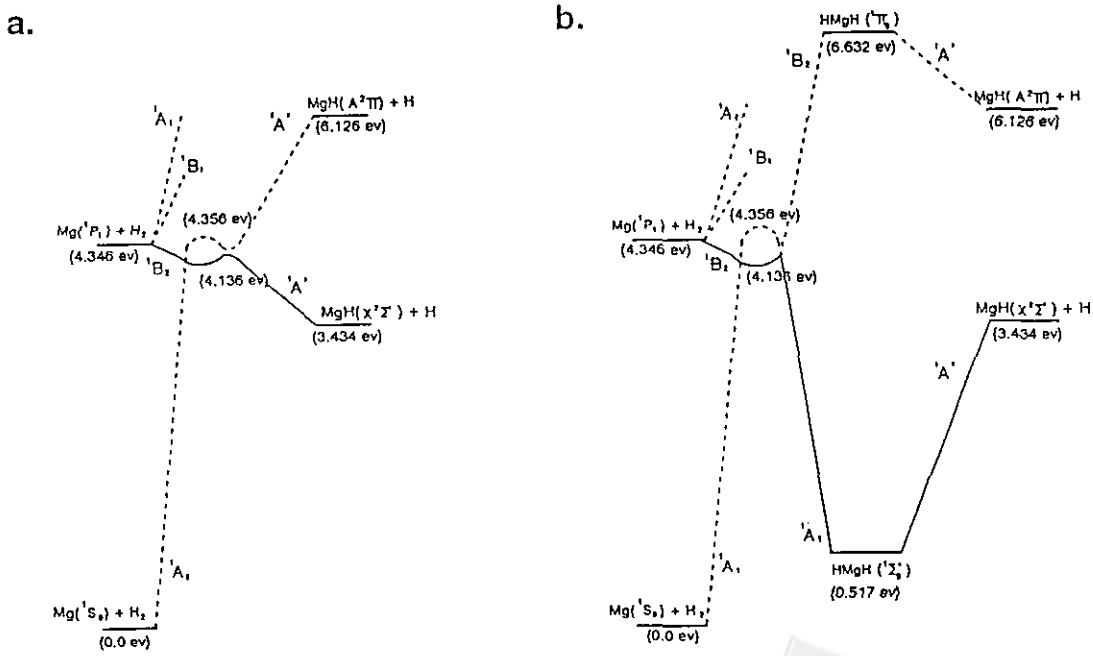

Fig. 9. (a) Reaction pathway that accounts for the experimental findings of MgH product in the low rotational states and preferentially $v'' = 0$. The bent intermediate near the surface crossing region follows the dissociation direction of Mg-H distance, leading to a weak angular dependence of the relevant PES. (b) Reaction pathway that accounts for the findings of the MgH product in the high rotational states and comparable vibrational population between $v'' = 0$ and 1. The intermediate near the surface crossing passes through a linear geometry before breaking apart, leading to a strong angular dependence of the relevant PES. For both pathways,the state energies relative to the Mg($^1S_0$) + H_2 reactants are calculated with a MP4/6-31G** method. The intermediate MgH_2 with bending angle at 50° is calculated near the crossing region.

with HD, is insignificant. The H-H bond elongates and begins to dissociate when the excited Mg atom approaches in the bent configuration, such that the H-H distance of the MgH_2 intermediate at the crossing region reaches a value between 1.5 and 2.2 Å, much larger than 0.74 Å in the equilibrium position. When one H atom (or D atom) departs, the force exerted directly on the other H atom is apparently negligible. This fact accounts for the lack of isotope effect. On the other hand, since the two parallel reaction mechanisms, responsible for the rotational bimodality, originate from the same intermediate at the crossing region, and in turn follow a distinct exit-channel coordinate, they should respond to an identical temperature dependence as observed.

CONCLUSION

The temperature dependence of MgH rotational state distribution demonstrates that the rotational bimodality observed in the reaction of $Mg(^1P_1)$ with H_2 results from the Mg-insertive, exit-channel controlled reaction. The conclusion is consistent with the isotope effect. With measurement of the rotational and vibrational population distribution of MgH(v″ = 0 and 1), two parallel reaction pathways are found to be responsible for the subject reaction. One mechanism causes the resulting MgH populated in the low rotational levels and preferentially v″ = 0, and the other mechanism produces MgH in higher rotational levels with comparable v″ = 0 and v″ = 1 populations. By means of the relevant PES information, we may successfully account for the reaction pathways involved. A nonadiabatic transition between the excited $^1B_2$ PES and the ground PES needs to take part in the reaction in order to obtain MgH in the $^1\Sigma^+$ state. The intermediate near the surface crossing, which follows directly the dissociation coordinate of the Mg-H distance, may produce MgH in low rotational states and preferentially v″ = 0 (Fig. 10a). In contrast, the intermediate which is attracted to pass a linear geometry may lead to rotational and vibrational excitation of MgH product (Fig. 10b). The isotope effect and the temperature dependence of MgH are also well explained with use of the calculated PES's.

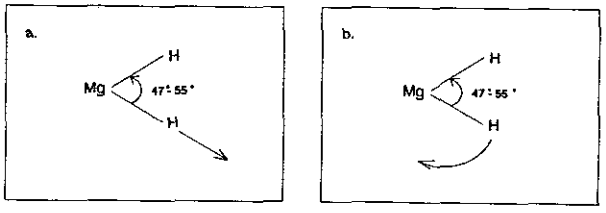

Fig. 10. (a) The removal of H from the intermediate MgH_2 near the surface crossing, casuing MgH populated in low rotational levels and preferentially v″ = 0. (b) The removal of H from the intermediate,causing MgH populated in higher rotational levels and comparable v″ = 0 and v″ = 1 population.

ACKNOWLEDGMENT

The authors wish to thank Professors W. H. Breckenridge, S. H. Lin, C. Wittig and K. Liu for their helpful discussions. The work is financially supported by the National Science Council of the Republic of China under the contract no.NSC84-2113-M-001-031.

Received January 7, 1995.

Key Words

Reaction pathway; Abstraction; Insertion; Temperature effect; Potential energy surface; Rotational population distribution; Vibrational population distribution.

REFERENCES

1. Breckenridge, W. H.; Umemoto, H. *In Dynamics of the Excited State*; Lawley, K. P. Ed.; Wiley: New York, **1982**; p 325.
2. Adams, N.; Breckenridge, W. H.; Simon, J. *Chem. Phys.* **1981**, *56*, 327.
3. Chaquin, P.; Sevin, A.; Yu, H. *J. Phys. Chem.* **1985**, *89*, 2813.
4. Liu, D. K.; Ou, Y. R.; Lin, K. C. submitted for publication.
5. Breckenridge, W. H.; Nikolai, W. L. *J. Chem. Phys.* **1980**, *73*, 2763.
6. Breckenridge, W. H.; Stewart, J. *J. Chem. Phys.* **1982**, *77*, 4469.
7. Breckenridge, W. H.; Umemoto, H. J. *Chem. Phys.* **1981**, *75*, 698.
8. Breckenridge, W. H.; Umemoto, H. J. *Chem. Phys.* **1984**, *80*, 4168.
9. Breckenridge, W. H.; Wang, J. H. *Chem. Phys. Lett.* **1987**, *137*, 195.
10. Lin, K. C.; Huang, C. T. *J. Chem. Phys.* **1989**, *91*, 5387.
11. Kleiber, P .D.; Lyyra, A. M.; Sando, K. M.; Zafiropulos, S. V.; Stwalley, W. C. *J. Chem. Phys.* **1986**, *85*, 5493.

12. Kleiber, P. D.; Lyyra, A. M.; Sando, K. M.; Heneghan, S. P.; Stwalley, W. C. *Phys. Rev. Lett.* **1985**, *54*, 2003.
13. McCaffery, J. G.; Parnis, J. M.; Ozin, G. A.; Breckenridge, W. H. *J. Chem. Phys.* **1985**, *89*, 4945.
14. Liu, D. K.; Chin, T. L.; Lin, K. C. *Phys. Rev. A* **1994**, *50*, 4891.
15. Breckenridge, W. H.; Malmin, O. K.; Nikolai, W. L.; Oba, D. *Chem. Phys. Lett.* **1978**, *59*, 38.
16. Levine, R. D.; Bernstein, R. B. In *Molecular Reaction Dynamics and Chemical Reacitvity*; Oxford University: Oxford, **1987**; pp 46-58.
17. Lin, K. C.; Chang, H. C. *J. Chem. Phys.* **1989**, *90*, 6151.
18. Wang, K. C.; Lin, K. C.; Luh, W. T. *Chem. Phys. Lett.* **1992**, *188*, 37.
19. Frisch, M. J.; Head-Gordon, M.; Trucks, G. W.; Foresman, J. B.; Schlegel, H. B.; Raghavachari, K.; Robb, M. A.; Binkley, J. S.; Gonzalez, C.; DeFrees, D. J.; Fox, D. J.; Whiteside, R. A.; Seeger, R.; Melius, C. F.; Baker, J.; Martin, R. L.; Kahn, L. R.; Stewart, J. J. P.; Topiol, S.; Pople, J. A. Gaussian 92.
20. Khan, M. A. *Proc. Phys. Soc. London* **1982**, *80*, 209.
21. Ahlrichs, R.; Keil, F.; Lischka, H.; Kutzelnigg, W.; Staemmler. J. *Chem. Phys.* **1975**, *63*, 455.
22. Francl, M. M.; Pietro, W. J.; Hehre, W. J.; Binkley, J. S.; Gordon, M. S.; DeFrees, D. J.; Pople, J. A. J. *Chem. Phys.* **1982**, *77*, 3654.
23. Herzberg, G. In *Molecular Spectra and Molecular Structure I: Spectra of Diatomic Molecules*; Second Edition; van Nostrand Reinhold, New York, **1950**; Chap. 5.
24. Earls, L. T. *Phys. Rev.* **1935**, *48*, 423.
25. Levine, R. D.; Bernstein, R. B. In *Molecular Reaction Dynamics and Chemical Reacitvity* ;Oxford University: Oxford, **1987**; Chap. 5.
26. Lin, S. H. (private communication).
27. Fairchild, P. W.; Smith, G. P.; Crosley, D. R. *J. Chem. Phys.* **1983**, *79*, 1795.
28. Rensberger, K. J.; Jeffries, J. B.; Crosley, D. R. *J. Chem. Phys.* **1989**, *90*, 2174.
29. Tsukiyama, K.; Katz, B.; Bersohn, R. *J. Chem. Phys.* **1985**, *83*, 2889.
30. Perry, D. S.; Polanyi, J. C. *Chem. Phys.* **1976**, *12*, 37.
31. Berry, M. J. *J. Chem. Phys.* **1973**, *59*, 6229.
32. Schinke, R. In *Photodissociation Dynamics*; Cambridge University press: Cambridge, **1993**.
33. Huber, J. R.; Schinke, R. *J. Phys. Chem.* **1993**, *97*, 3463.